

Analysis of Grid Connected DFIG based Wind Farms for Reactive Power Compensation

S.Janarthanan

Assistant Professor, Department of EEE, AMET University, Chennai, Tamil Nadu, India

Abstract— The proposal of this project addresses the reactive power generation of offshore wind parks using double fed induction generators (DFIG) connected to the main grid with long cables. During steady state operation, reactive power can be generated with minimum power loss of wind energy system while meeting the grid code requirement. During grid disturbance, the wind power generators have to provide voltage support by increasing reactive current supply. DFIG are the machines of choice for large wind turbines. The doubly fed induction generator system is investigated as viable alternative to adjust speed over a wide range while keeping cost of the power converters minimal. Decoupled control of active and reactive power can be realized using the dynamic model of the DFIG. The modeling and control of DFIG and the simulation was done in MATLAB Simulink environment and the results are verified.

Keywords—Double fed induction generator, Wind turbine, Grid fault, Reactive power generation.

I. INTRODUCTION

Electrical power can be alternatively generated by renewable energy. There are various renewable energy sources available and one of the well advanced sources is wind energy also commonly used for generating electrical power. Wind energy is converted into electrical power using wind turbine (WTs) and it can be operated at either fixed (or) variable speed. The generated of the fixed and variable speed wind turbines are controlled by electrical grid and power electronic equipment respectively.

The Variable speed wind turbines are most commonly used because it has characteristics of noise reduction, active and reactive power control and reduction of mechanical [8].

In recent years, for large wind turbines double-fed induction generators are mostly used by industries. Double-fed induction generator has the advantage of handling fraction (20-30%) of the total power by its power electronic equipment, which made its very popular.

In direct-driven synchronous generator the power electronic equipment has to handle the total system power so the losses in its power electronic equipment can be higher than the double- fed induction generator.

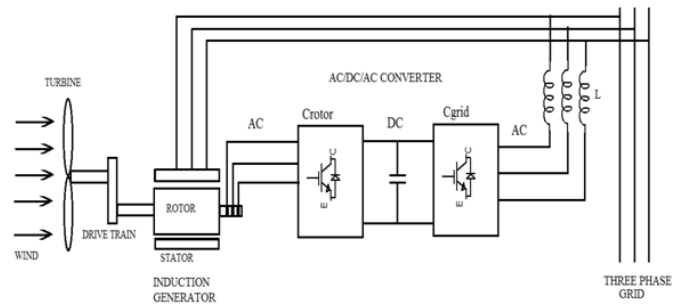


Fig.1. Wind turbine based DFIG.

So, the main objective of this paper is

- To study reactive power performance of the DFIG under steady state and transients conditions.
- DFIG operation for variable speed and its corresponding capacity towards the reactive power control.

In this paper presents real and reactive power control of DFIG during normal and faulty conditions. Integration of wind energy into existing power systems leads to various power quality problems. During grid faults DFIG can able to inject reactive power to the grid.

II. DOUBLE FED INDUCTION GENERATOR

The A standard double fed induction generator consists of wound rotor induction machine and IGBT-based PWM converter. The stator and rotor windings of the doubly fed induction generator is connected to the 50Hz grid through AC/DC/AC convertor connected to rotor winding and DC/AC converter connected to grid is called grid side convertor.

The main application of double-fed induction generator (DFIG) is the high-power wind application. DFIG has an advantage of control rotor current flows which leads to two main functions namely reactive power control and variable speed operation. By this featured it can works at the wide range of the wind speeds with maximum efficiency. The AC/DC/AC conversion is normally PWM convertors, which reduces the harmonics, present in the wind turbines driven DFIG system using sinusoidal PWM technique. Here C_{rotor} represents rotor side convertor and C_{grid} represents grid side convertor. The speed of the wind turbine can be controlled by electronic control (or) gear boxes.

The main characteristics are

- Limited operating speed range (30% to 20%).
- Small scale power electronic converter (reduced power losses and price).
- Active power and reactive power control exchanged with grid.
- Need for slip-rings.
- Need for gearbox (normally a three-stage one).

III. DYNAMIC MODELING OF THE DFIG

The compact set of model differential equation represents the dynamic modeling of DFIG. The dynamic modeling can be simulated using computer based software and the information deals with machine variables are provided.

Fig.1 represents the simplified model of DFIM with three winding stator and three winding rotor which represents the real machine. By this the equivalent circuit model can be derived and the following equation represents the instantaneous stator voltages, current and fluxes of the machine respectively.

$$v_{as}(t) = R_s i_{as}(t) + \frac{d\psi_{as}(t)}{dt} \rightarrow (1)$$

$$v_{bs}(t) = R_s i_{bs}(t) + \frac{d\psi_{bs}(t)}{dt} \rightarrow (2)$$

$$v_{cs}(t) = R_s i_{cs}(t) + \frac{d\psi_{cs}(t)}{dt} \rightarrow (3)$$

where R_s is the stator resistance; $i_{as}(t)$, $i_{bs}(t)$, and $i_{cs}(t)$ represents the a, b, c phases of stator current, $v_{as}(t)$, $v_{bs}(t)$, and $v_{cs}(t)$ represents the voltage applied for stator, and $\psi_{as}(t)$, $\psi_{bs}(t)$, and $\psi_{cs}(t)$ denotes the stator fluxes.

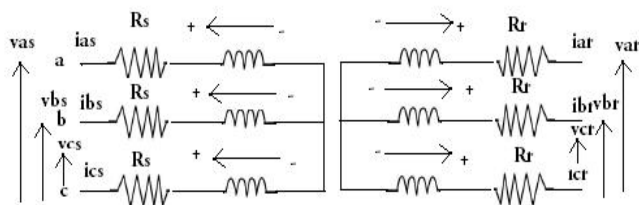


Fig.2. DFIG electric equivalent circuit.

Similarly, the magnitudes of rotor are

$$v_{ar}(t) = R_r i_{ar}(t) + \frac{d\psi_{ar}(t)}{dt} \rightarrow (4)$$

$$v_{br}(t) = R_r i_{br}(t) + \frac{d\psi_{br}(t)}{dt} \rightarrow (5)$$

$$v_{cr}(t) = R_r i_{cr}(t) + \frac{d\psi_{cr}(t)}{dt} \rightarrow (6)$$

where R_r represents the rotor resistance referred to stator, $i_{ar}(t)$, $i_{br}(t)$ and $i_{cr}(t)$ represents the stator referred rotor currents of phases a, b, c; $v_{ar}(t)$, $v_{br}(t)$ and $v_{cr}(t)$ denotes the stator referred rotor voltages, and $\psi_{ar}(t)$, $\psi_{br}(t)$ and $\psi_{cr}(t)$ indicates the rotor fluxes. Rotor magnitudes have constants angular frequency when its operates under steady state conditions.

The stator and rotor angular frequency can be related as follows,

$$\omega_r + \omega_m = \omega_s \rightarrow (7)$$

$$\omega_m = p\Omega_m \rightarrow (8)$$

A. Synchronously Rotating References Frames

The model of the DFIM is represented by the differential equation which is derived by using the space vector notation in the synchronous reference frame.

The following equations (9) and (10) represent the stator and rotor voltage equations

$$\vec{v}_s^a = R_s \vec{i}_s^a(t) + \frac{d\vec{\psi}_s^a}{dt} + j\omega_s \vec{\psi}_s^a \rightarrow (9)$$

$$\vec{v}_r^a = R_r \vec{i}_r^a(t) + \frac{d\vec{\psi}_r^a}{dt} + j(\omega_s - \omega_m) \vec{\psi}_r^a \rightarrow (10)$$

$$\omega_s - \omega_m = \omega_r \rightarrow (11)$$

In these equations, the superscript “a” indicates the space vectors referred to a synchronously rotating frame.

$$\vec{\Psi}_s^a = L_s \vec{i}_s^a + L_m \vec{i}_r^a \rightarrow (12)$$

$$\vec{\Psi}_r^a = L_m \vec{i}_s^a + L_r \vec{i}_r^a \rightarrow (13)$$

Under the steady state condition, when the sinusoidal voltages are supplied there will be constant values of dq components of the voltages, currents, and fluxes. This is contrast to the $\alpha\beta$ components that are sinusoidal magnitudes.

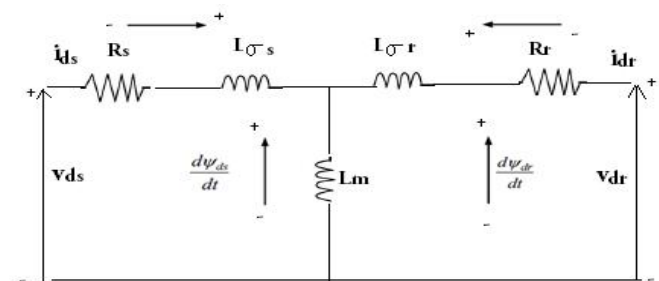


Fig.3. Dynamic d^e axis circuit.

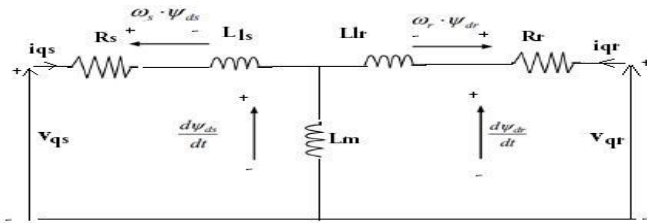


Fig.4. Dynamic q^c axis circuit.

Fig.3 and Fig.4 represents the dq equivalent circuit model of the DFIG, in synchronous coordinates.

The power expressions in the dq reference frame and the $\alpha\beta$ equation are equivalent

$$P_s = \frac{3}{2} \text{Re} \{ \vec{v}_s \cdot \vec{i}_s^* \} = \frac{3}{2} \{ v_{ds} i_{ds} + v_{qs} i_{qs} \} \rightarrow (14)$$

$$P_r = \frac{3}{2} \text{Re} \{ \vec{v}_r \cdot \vec{i}_r^* \} = \frac{3}{2} \{ v_{dr} i_{dr} + v_{qr} i_{qr} \} \rightarrow (15)$$

$$Q_s = \frac{3}{2} \text{Re} \{ \vec{v}_s \cdot \vec{i}_s^* \} = \frac{3}{2} \{ v_{qs} i_{ds} - v_{ds} i_{qs} \} \rightarrow (16)$$

$$Q_r = \frac{3}{2} \text{Re} \{ \vec{v}_r \cdot \vec{i}_r^* \} = \frac{3}{2} \{ v_{qr} i_{dr} - v_{dr} i_{qr} \} \rightarrow (17)$$

The torque equation is given as,

$$T_{em} = \frac{3}{2} P \frac{L_m}{L_s} I_m \{ \vec{\Psi}_s \cdot \vec{i}_r^* \} = \frac{3}{2} P \frac{L_m}{L_s} \{ \vec{\Psi}_{qr} i_{dr} - \vec{\Psi}_{dr} i_{qr} \} \rightarrow (18)$$

IV. DOUBLY FED INDUCTION GENERATOR UNDER FAULT

The stator voltage and flux start down to zero when the 3-phase fault occurs. The voltage drops are depends upon the location of the fault. Then the rotor current increases lead to maintain the flux linkage within the rotor windings constant.

In this case, the two factors namely change in the stator flux and change in rotor injected voltage determines the increases in the rotor current suddenly after a fault in the DFIG.

A. Behavior immediately after the fault

When the fault occurs immediately there is a drop of voltage at the DFIG generator terminal which causes the decrease of stator and rotor flux of the generator. The decreases in the stator flux leads to the release of magnetization which stored in the magnetic field and its denoted in Fig.9, by the reactive power peak in the moment of fault [6], [7].

High current transients will appear in the stator and rotor winding at the time of fault. Increases in the rotor current can be compensated as the rotor side converter increases the rotor voltage reference, which leads to the “rush” of power from the rotor terminals through converter. In the another side, after the fault instant grid voltage has dropped, and the transformation of the whole power from the rotor through the converter

further to the grid cannot done by the grid side and the control of the dc-voltage by the grid side converters quickly reaches its limitation.

Finally, the dc-voltage rises rapidly because of charging the dc-bus capacitor when addition energy goes into it.

B. Behavior of fault clearance

At the time of fault, the rotor speed has been increases as the reduction n the stator voltage and rotor flux and the changes in injected rotor voltage. The fault is cleared. Immediately, the stator voltage is restored, and the increase in the stator and rotor currents occurs when the demagnetized stator and rotor oppose this change in flux [8].

V. SIMULATION RESULTS

A. Doubly fed induction generator under normal condition

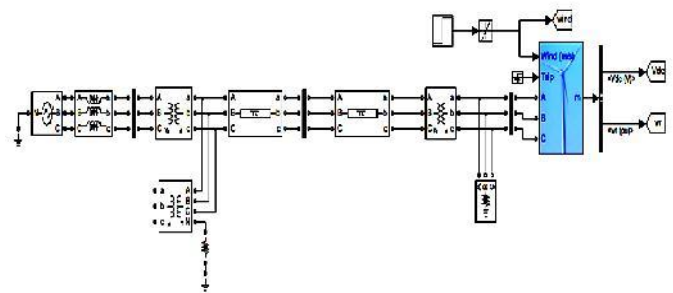


Fig.5. Double Fed Induction Generator under Normal Condition.

Fig.5 represents the simulation model of DFIG under normal condition. A 9MW wind farm consisting of six 1.5MW wind turbine connected to a 25kv distribution system exports power to a 120kv grid through a 30km, 25kv feeder. Wind turbines use a DFIG consisting of a wound rotor induction generator and Ac/Dc/Ac/ IGBT base PWM converter.

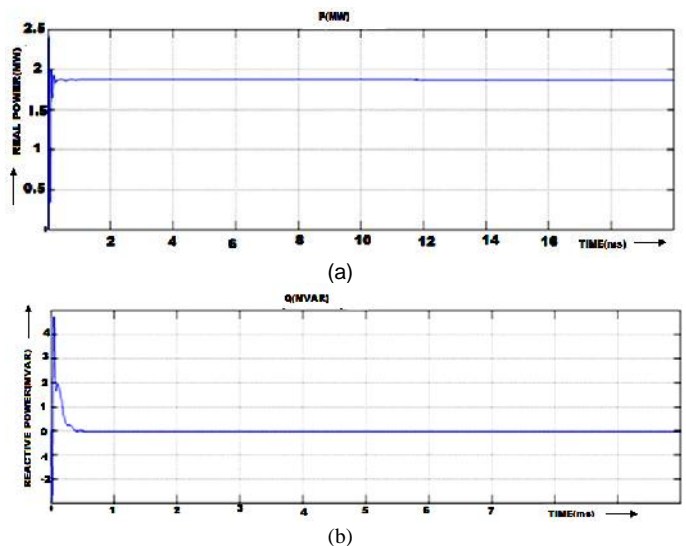


Fig.6. Real and Reactive power of DFIG.

During normal condition real and reactive power does not changes across the grid. The real power is maintain constant at 1.87MW and reactive power is -0.04177Mvar shown in Fig 6.

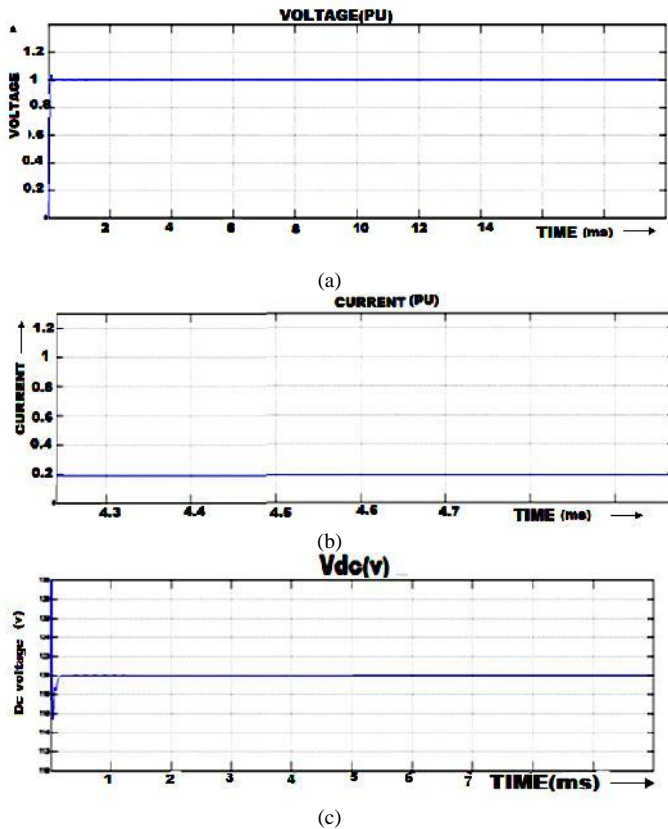


Fig.7. Voltage, Current and Dc link voltage of DFIG.

Similarly, under normal condition DFIG will be maintained constant voltage and current. Dc link voltage maintain constant at 1200V shown in Fig7.

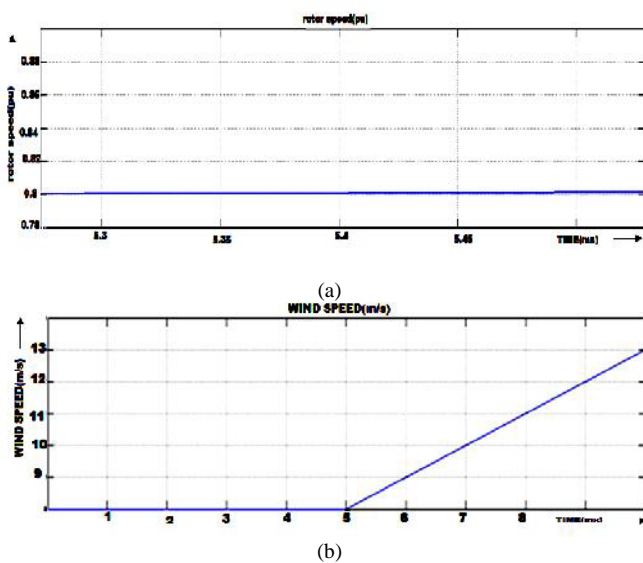


Fig.8. Rotor and Wind speed of DFIG.

Rotor and wind speed of DFIG under normal condition shown in Fig 8. The rotor speed is maintained constant 0.8926 pu and wind speed varies after 5ms. The initial speed is set at 8m/s and final speed is 14m/s.

B. Double Fed Induction Generator under Fault Condition

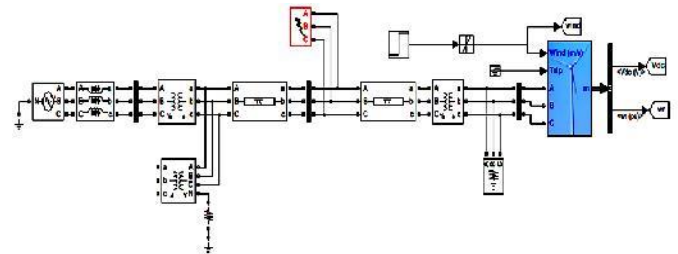


Fig.9. Double Fed Induction Generator under Fault Condition.

Fig.9 represents the simulation model of DFIG under fault condition. A 9MW wind farm consisting of six 1.5MW wind turbine connected to a 25kv distribution system. In this 3-phase fault will be connected across 25 km transmission line. And set the internal control time 5ms.

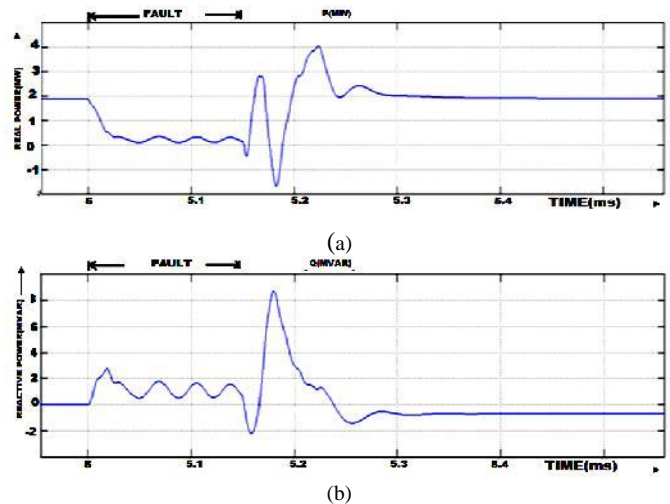
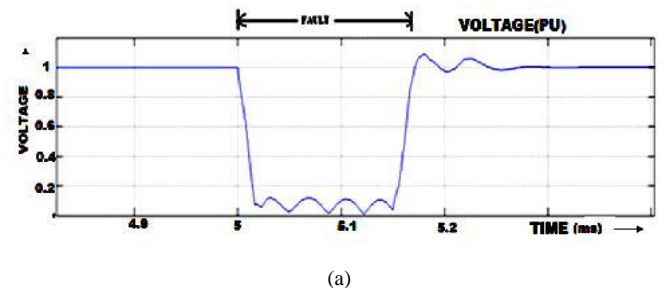


Fig.10. Real and Reactive power of DFIG.

During fault condition real power decreases 2.624 MW to -0.5 and Reactive power decreases -0.3576 Mvar to -3.11Mvar across the grid up to 5 to 5.15m/s period. In that time DFIG injects 8.61Mvar reactive power to the grid shown in fig10. After the fault period the power will be return to normal operation. The fault clearance time is after 5.15m/s.



(a)

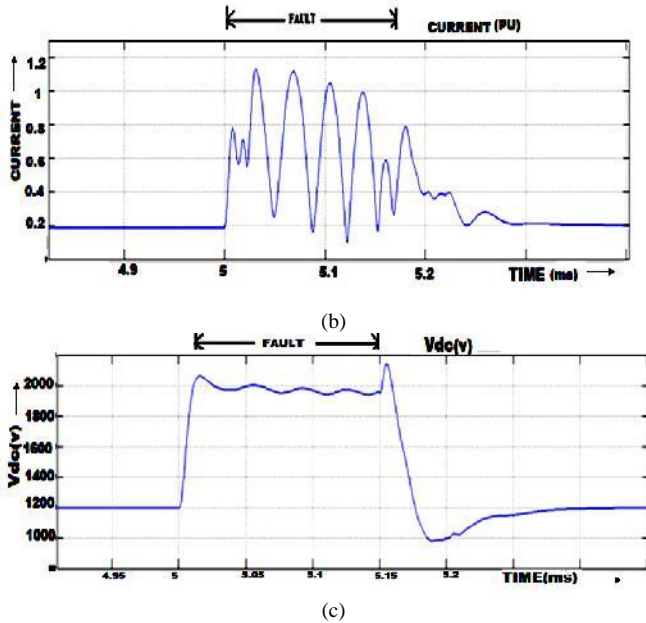


Fig.11. Voltage, Current and Dc link voltage of DFIG.

During fault condition voltage decreases 1.001pu to 0 and current suddenly increases 0.2642 to 1.135 across the grid up to 5 to 5.15m/s period. Similarly dc link voltage also increases. In that time DFIG injects 8.61Mvar reactive power to the grid. After the fault period it will be return to normal operation. The fault clearance time is after 5.15m/s shown in fig11.

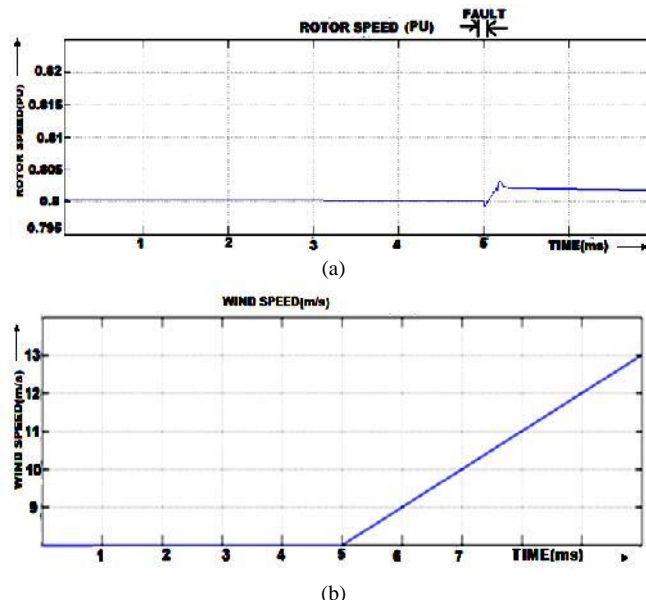


Fig.12. Rotor and Wind speed of DFIG.

Rotor and wind speed of DFIG under fault condition shown in fig 12. The rotor speed is decreases 0.8946 to 0.7993 pu and returns to normal operation after the fault clearance time. Wind speed is varies after 5ms. The initial speed is set at 8m/s and final speed is 14m/s.

C. DFIG for Variable Speeds

S.No	Wind Speeds	Parameter	Fault Condition Values
1.	5m/s	Real Power	2.624 MW
		Reactive Power	-0.3576 Mvar
		Rotor Speed	0.8945 pu
2.	8m/s	Real Power	2.005 MW
		Reactive Power	-0.2626Mvar
		Rotor Speed	0.8184 pu
3.	12m/s	Real Power	2.001MW
		Reactive Power	-0. 2429Mvar
		Rotor Speed	0.8369 pu

Table.1. Output summary of DFIG for variable speeds

VI. CONCLUSION

In this paper has presented the modeling and simulation of wind turbine driven doubly fed induction generator which feeds to power to the utility grid. DFIG model has been described based on the dynamic approach and this model can be applicable for all types of induction generator configurations for steady state and transient analysis. During grid fault condition voltage stability problem will occurs across the grid. To overcomes this voltage stability problem DFIG able to adjust reactive power to the grid. And if the wind speeds varies it does not affects the generator power and the injection voltage will be same under fault period

REFERENCES

- [1]. A. H. Kasem, E. F. El-Saadany, H. H. El-Tamaly, and M. A. A. Wahab, "A new fault ride through strategy for doubly fed wind-power induction generator," in Proc. IEEE Elect. Power Conf., Canada, 2007, pp. 1-7.
- [2]. J. Lopez, P. Sanchis, X. Robom, and L. Marroyo, "Dynamic behavior modeling of the doubly fed induction generator during three-phase voltage dips," IEEE Trans. Energy Convers., vol. 22, no. 3, pp. 709-717, Sep.2007.
- [3]. O. Abdel-Baqi and A. Nasiri, "A dynamic LVRT solution for doubly fed induction generator," IEEE Trans. Power Electron., vol. 25, no. 1, pp. 193-196, Jan.2010.
- [4]. J. A. Suul, M. Molinas, and T. Underland, "STATCOM based indirect torque control of induction machine during voltage recovery after grid fault," IEEE Trans. Power electron. vol. 25, no. 5, pp. 1240-1250, May 2010.
- [5]. J. B. Ekanayake, L. Holdsworth, X. G. Wu, and N. Jenkins, "Dynamic modeling of doubly fed induction generator wind turbines," IEEE Trans. power Syst., vol. 18, no. 2, pp. 803-809, May 2003.
- [6]. J.Morren and S.W. H. de Haan, "Ride through of wind turbines with doubly-fed induction generator during a voltage dips," IEEE Trans. Energy Convers., vol. 20, no. 2, pp. 435-441, Jun 2005.
- [7]. M. Kayikei and J. Milanovic, "Reactive power control strategies for DFIG-based plants," IEEE Trans. Energy Convers., vol. 22, no. 2, pp. 389-396, Jun 2007.
- [8]. C. Eisenhut, F. Krug, C. Schram, and B. Klockl, "Wind-turbine model for system simulations near cut-in-speed," IEEE Trans. Energy convers., vol. 22, no.2, pp. 421-430, Jun 2007.